LJMU Research Online

Makin, ADJ, Piovesan, A, Tyson-Carr, J, Rampone, G, Derpsch, Y and Bertamini, M

 Electrophysiological priming effects confirm that the extrastriate symmetry network is not gated by luminance polarity

http://researchonline.ljmu.ac.uk/id/eprint/14070/

Article

For more information please contact researchonline@ljmu.ac.uk

RESEARCH REPORT

EJN European Journal of Neuroscience   FENS   WILEY

Electrophysiological priming effects confirm that the extrastriate symmetry network is not gated by luminance polarity

Alexis D. J. Makin[1] [iD] | **Andrea Piovesan**[2] | **John Tyson-Carr**[1] | **Giulia Rampone**[1] | **Yiovanna Derpsch**[1] | **Marco Bertamini**[1]

[1]Department of Psychological Sciences, University of Liverpool, Liverpool, United Kingdom

[2]Department of Psychology, Edge Hill University, Ormskirk, United Kingdom

Correspondence
Alexis D. J. Makin, Department of Psychological Sciences, Eleanor Rathbone Building, University of Liverpool, Liverpool, Merseyside L69 7ZA, United Kingdom.
Email: Alexis.makin@liverpool.ac.uk

Funding information
Economic and Social Research Council, Grant/Award Number: ES/S014691/1

Abstract

It is known that the extrastriate cortex is activated by visual symmetry. This activation generates an ERP component called the Sustained Posterior Negativity (SPN). SPN amplitude increases (i.e., becomes more negative) with repeated presentations. We exploited this *SPN priming effect* to test whether the extrastriate symmetry response is gated by element luminance polarity. On each trial, participants observed three stimuli (patterns of dots) in rapid succession (500 ms. with 200 ms. gaps). The patterns were either symmetrical or random. The dot elements were either black or white on a grey background. The triplet sequences either showed repeated luminance (black > black > black, or white > white > white) or changing luminance (black > white > black, or white > black > white). As predicted, SPN priming was comparable in repeated and changing luminance conditions. Therefore, symmetry with black elements is not processed independently from symmetry with white elements. Source waveform analysis confirmed that this priming happened within the extrastriate symmetry network. We conclude that the network pools information across luminance polarity channels.

KEYWORDS

luminance polarity, reflection, regularity, repetition enhancement, sustained posterior negativity

1 | INTRODUCTION

Visual symmetry has been studied extensively (Bertamini, Silvanto, Norcia, Makin, & Wagemans, 2018; Cattaneo, 2017; Treder, 2010). Symmetry is an important cue for object recognition and figure-ground segmentation (Driver, Baylis, & Rafal, 1992; Koffka, 1935). Here we consider reflectional (mirror) symmetry only, although it not the only type (Mach, 1886). In reflectional symmetry, there is a correlation between element position on either side of the axis (Barlow & Reeves, 1979). Therefore models of symmetry perception consider how local element position signals are integrated to

---

form a global gestalt (van der Helm & Leeuwenberg, 1996; Wagemans, Van Gool, Swinnen, & Vanhorebeek, 1993).

Early vision can be conceptualized as a retinotopic array of spatial frequency and orientation tuned filters (Campbell & Robson, 1968). Building on this foundation, *filter models* presume that the first stage in symmetry perception involves low-pass filtering of the image. This extracts midpoint-co-linear blobs that are aligned orthogonally to any axes of reflection. Symmetry discrimination can then proceed by estimating blob alignment (Dakin & Hess, 1997; Dakin & Watt, 1994; Osorio, 1996). Dakin and Hess (1998) suggest that symmetry is extracted in this way from a narrow integration window elongated about the axis. Julesz and Chang (1979) found that participants can ignore noise masks as long as they differ in spatial frequency from the underlying symmetrical pattern. Likewise, Rainville and Kingdom (2000) found that participants can ignore noise masks with different orientations. These considerations suggest specific symmetry representations are linked to specific spatial frequency filters. Therefore, different symmetry representations may *not* overlap and perceptually interfere with each other.

Reflected elements can vary in their low-level visual properties, such luminance or colour. To accommodate these variations, filter models sometimes incorporate a full or half wave rectification stage at the front end (e.g. Dakin & Hess, 1997). Among other things, such rectification eliminates the difference between black and white elements on a grey background. Global integration can then utilize contrast signals rather than luminance signals. Early half-wave rectification is also incorporated into some influential shape detection models (Poirier & Wilson, 2010; Wilson & Wilkinson, 2002). These considerations suggest that there should be complete overlap between symmetry representations with different luminance polarity (even if there is no overlap between symmetry representations with different spatial frequencies).

Furthermore, Glass pattern (Glass, 1969) aftereffects are known to transfer perfectly between black and white exemplars (Clifford & Weston, 2005). This again suggests that some types of global structure are coded independently of element luminance polarity. This could be true of reflectional symmetry as well.

Without referring to filter models directly, Tyler and Hardage (1996) also addressed these topics. They distinguished *first-order (luminance) mechanisms*, which only find symmetrical correspondences between elements of the same luminance polarity (and operate over short distances), and *second-order (contrast) mechanisms*, which can find symmetrical correspondences between elements of opposite luminance polarity (and can operate over long distances spanning the whole visual field). Tyler and Hardage (1996) measured symmetry sensitivity while varying density and eccentricity. If second-order mechanisms dominate, then symmetry sensitivity should improve at low densities, and this was indeed

the case. Tyler and Hardage (1996) also compared *matched luminance polarity* conditions (black regions paired with black, and white paired with white) and *opposite luminance polarity conditions* (white paired with black, and black paired with white). Symmetry detection could tolerate opposite luminance polarity when density was low. This again emphasises the role of second-order mechanisms. In light of these findings, Tyler and Hardage (1996) concluded that long-range, second-order mechanisms predominate in symmetry detection. This account again suggests reflectional symmetry is coded independently of element luminance polarity.

Opposite luminance polarity symmetry is often termed anti-symmetry. Symmetry and anti-symmetry are sometimes perceptually equivalent, as found by Tyler and Hardage (1996). However, there are many cases where anti-symmetry is perceptually weaker. For instance, anti-symmetry discrimination declines at high element density, when multiple greyscale levels are used, and when elements are presented in the periphery (Mancini, Sally, & Gurnsey, 2005; Wenderoth, 1996). It seems that global symmetry detection mechanisms are *sensitive* to luminance polarity (mis)matching across the axis. Apparently, early filter-rectification and/or second order mechanisms do not *always* render black and white elements informationally identical and thereby abolish *all* anti-symmetry costs.

Following these themes, Gheorghiu, Kingdom, Remkes, Li, and Rainville (2016) tested whether symmetry perception is *selective* for low-level properties: For example, are symmetrical arrangements of black dots coded by one neural mechanism, and symmetrical arrangements of white dots coded by another neural mechanism? In other words, we can ask whether symmetry perception mechanisms are *gated* by luminance polarity. Wright, Mitchell, Dering, and Gheorghiu (2018) presented evidence against selectivity. They claimed that "symmetry detection mechanisms pool both luminance-polarities into one channel, and thus, extrastriate visual areas sensitive to symmetry are not gated by luminance polarity" (page 487). This non-selectivity hypothesis is partially anticipated by the work mentioned above, such as the second-order predominance account of Tyler and Hardage (1996), and filter models with an early rectification stage (Dakin & Hess, 1997). For simplicity, we use the term non-selectivity hypothesis to refer to this family of related ideas.

The current project tested the non-selectivity hypothesis. We measured an established ERP called the Sustained Posterior Negativity (SPN): After 200 ms, amplitude is lower at posterior electrodes when participants view symmetrical compared to asymmetrical stimuli. This posterior negativity was first identified by Norcia, Candy, Vildavski, and Tyler (2002), and has been replicated many times (Jacobsen & Höfel, 2003; Makin, Rampone, Morris, & Bertamini, 2020; Makin, Wilton, Pecchinenda, & Bertamini, 2012; Makin et al., 2016). Source localization shows that the SPN is generated in the extrastriate cortex.

This is consistent with fMRI work, which has identified symmetry activations in a network of extrastriate regions, including V4 and the shape-sensitive Lateral Occipital Complex (LOC). This extrastriate symmetry response was first found in an fMRI study by Tyler et al. (2005), and then replicated by others (Keefe et al., 2018; Kohler, Clarke, Yakovleva, Liu, & Norcia, 2016; Sasaki, Vanduffel, Knutsen, Tyler, & Tootell, 2005; Van Meel, Baeck, Gillebert, Wagemans, & Op de Beeck, 2019). SPN localization is also consistent with TMS research, which has found that disruption of the LOC impairs symmetry detection (Bona, Cattaneo, & Silvanto, 2015; Bona, Herbert, Toneatto, Silvanto, & Cattaneo, 2014).

Recently, we found that SPN amplitude *increases* (that is, becomes more negative) with repeated presentation of symmetrical patterns (Bertamini, Rampone, Oulton, Tatlidil, & Makin, 2019). We term this repetition enhancement effect *SPN priming*. Following an established research strategy (e.g. Kim, Biederman, Lescroart, & Hayworth, 2009; Kourtzi & Kanwisher, 2001), our recent work has exploited SPN priming to assess the independence of different symmetry representations (Makin, Tyson-Carr, Rampone, Derpsch, & Bertamini, 2020). Experiment 1 of Makin, Tyson-Carr, et al. (2020) found SPN priming with repeated presentation of different exemplars, but not repeated presentation of identical exemplars (Figure 1). Other experiments in Makin, Tyson-Carr, et al. (2020) demonstrated that SPN priming survives changes in regularity type, but not changes in retinal location, or unpredictable changes in axis orientation. In the current work, we tested whether SPN priming would survive changes in element luminance polarity, as predicted by the non-selectivity account.

We used different exemplars (Figure 2), known to produce SPN priming (red wave in Figure 1). Following Makin, Tyson-Carr, et al. (2020), we used a secondary task that was unrelated to symmetry: Our participants discriminated between normal sequences with three patterns, and oddball sequences, with a blank in the middle (Figure 2b).

In the *Repeated luminance condition*, polarity was held constant across the three presentations in a trial (e.g. black > black > black or white > white > white). Conversely, in the *Changing luminance condition*, polarity alternated (e.g. black > white > black or white > black > white). The non-selectivity account predicts that SPN priming should be equivalent in both Repeated and Changing luminance conditions. These predictions were pre-registered (https://aspredicted.org/2rh7e.pdf).[1]

2 | METHOD

2.1 | Participants

Twenty-two participants were involved (mean age 20, range 18–50, 2 males, 1 left-handed). The pre-registered aim of testing 24 participants was abandoned prematurely due to the COVID19 pandemic. The experiment had local ethics committee approval and was conducted in accordance with the Declaration of Helsinki (2008).

2.2 | Apparatus

Participants sat 57 cm from a 29 × 51 cm LCD monitor, updating at 60Hz. A chin rest was used for head stabilization. EEG data was recorded continuously at 512 Hz from 64 scalp electrodes (BioSemi Active-2 system, Amsterdam, Netherlands). Horizontal and Vertical EOG external channels were used to monitor excessive blinking and eye movements. The experiment was programmed in Python using open source PsychoPy libraries (Peirce, 2007).
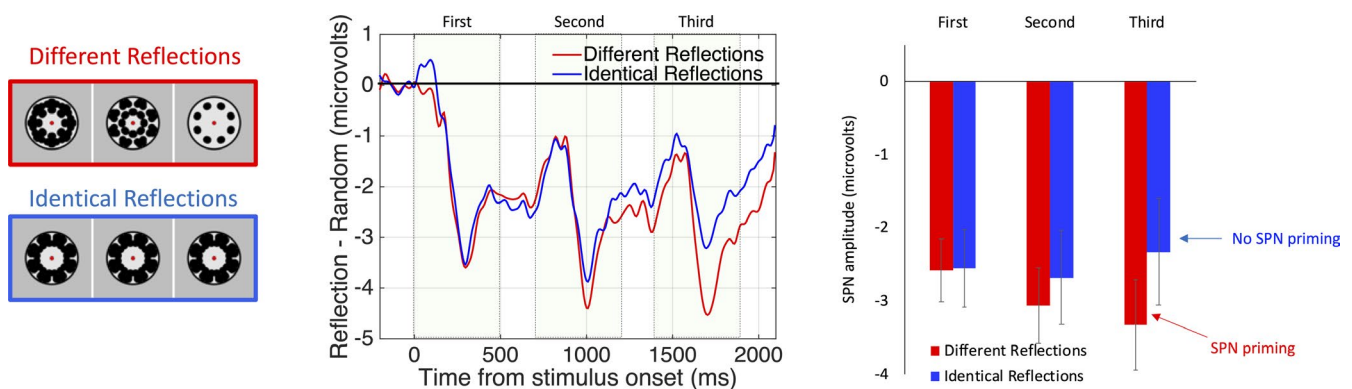
FIGURE 1 Selective SPN priming effect when novel exemplars are shown. Data from Makin, Tyson-Carr, et al. (2020). Participants viewed a sequence of three reflectional symmetries (left). The sequence could involve different reflections (red outline) or identical reflections (blue outline). The SPN was the difference between reflection and random waves (middle). SPN amplitude increased (i.e. became more negative) with repeated presentations of different reflections (red) but not with repeated presentations of the same reflection (blue). This is shown in the bar chart on the right (error bars = 95% CI)
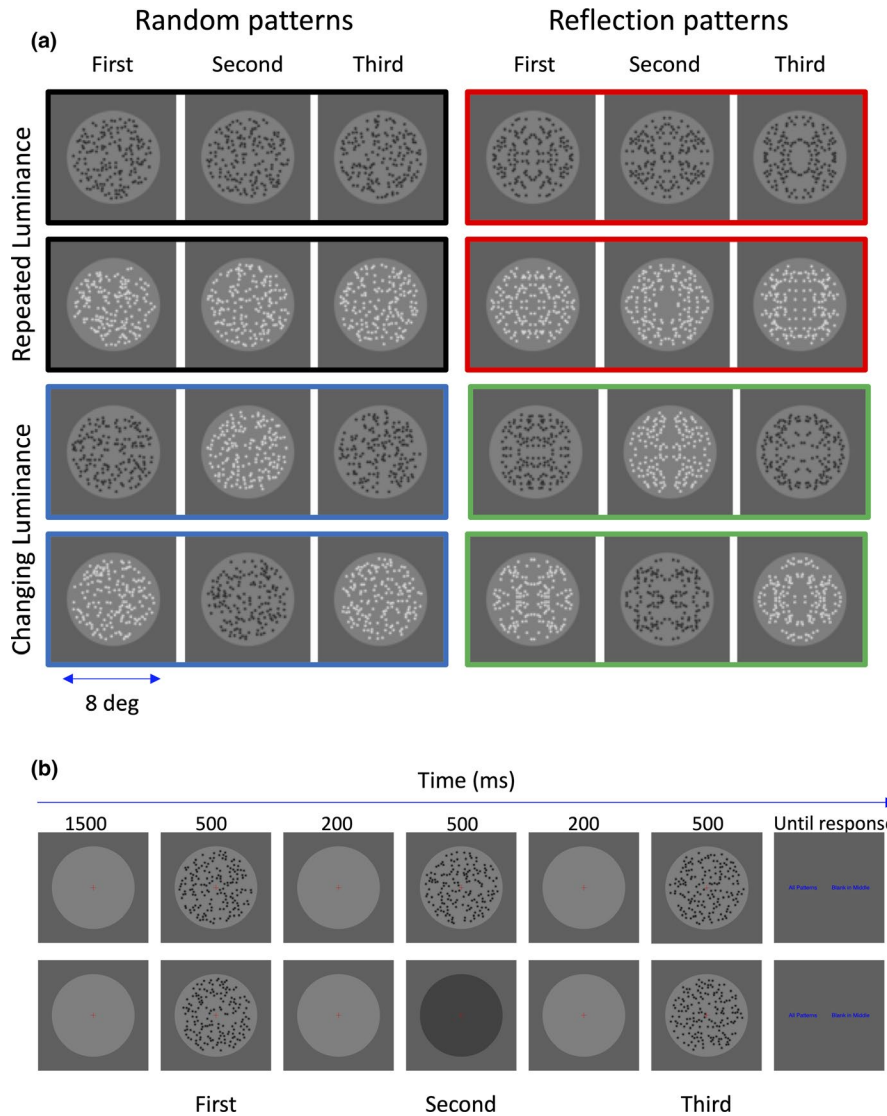
FIGURE 2 (a) Triplet sequences used in this experiment. Colour coding matches the ERP results in Figures 4 and 5. These are just examples, in the real experiment, every trial involved different patterns. (b) Example trial structure. The participant's task was to discriminate common "all pattern" trials, (top row, 80%) from infrequent "blank in the middle" trials (bottom row, 20%)

2.3 | Stimuli

Patterns were comprised of 160 non-overlapping black or white Gabor elements on a circular grey background. The circular disk was 8° in diameter. The regions where the elements could fall was 7.14° diameter. The visible dot at the centre of each circular Gabor was approximately 0.25 degrees diameter. In PsychoPy RGB coordinates (which vary from −1 to 1), the background was dark grey [−0.25, −0.25, −0.25], the circular region mid-grey [0, 0, 0], the black elements were black [−1, −1, −1] and the white elements were white [1, 1, 1]. Stimuli were generated offline and saved as PNG files. The reflection patterns had horizontal and vertical axes. We used 2-fold reflection in this study to increase signal strength (SPN amplitude almost doubles as we go up from 1 to 2 folds, e.g. Makin et al., 2016). All experiments used the same set of images, but these were shuffled so they played a different role in for each participant.

2.4 | Procedure

The timeline of a single trial was based on Makin, Rampone, Morris, et al. (2020). The 1,500 ms fixation baseline was followed by three 500 ms patterns with 200 ms gaps. In 80% of trials, all three presentations in the sequence were reflection or random patterns (Figure 2b top row). In the remaining 20% there was blank oddball between two random patterns (Figure 2b bottom row). The participant's task was to discriminate normal from oddball trials (by pressing buttons labelled "All patterns" or "Blank in the middle"). The response mapping switched between trials, so sometimes the left (A) key was used to report 'Blank in middle' and sometimes the right (L) key was used to report "Blank in middle."

Each participant completed 600 trials in total. 480 were normal trials, 120 were oddball trials. Only the normal trials were analysed. Of the 480 trials, there were 60 in each of the 8 triplet types shown in Figure 2a. There were thus 120 trials in

the 4 crucial conditions [(Reflection, Random) X (Repeated luminance, Changing luminance)]. The experiment was broken into 30 blocks of 20 trials. Within each block, conditions were presented in a randomized order. A single practice block was presented before the experiment began.

2.5 | ERP analysis (sensor level)

Pre-processing conventions were chosen a-priori and pre-registered. EEG data from 64 channels was analysed off-line using EEGLAB 13.3.4b toolbox in Matlab (Delorme & Makeig, 2004). The data were re-referenced to the scalp average, low pass filtered at 25Hz, downsampled to 128 Hz and segmented into −0.5 to +2.1 s epochs with a −200 ms pre-stimulus baseline. Eye blinks and other large artefacts were removed using Independent Components Analysis (Jung et al., 2000). An average of 10.05 (min 4, max 16) components were removed. Trials where amplitude exceeded ±100 microvolts were removed from all analysis (11%–12%). Oddball trials were not included in the ERP analysis. We did not remove ERP trials if participants entered an incorrect response because these infrequent mistakes probably happen during response entry and excluding error trials would make only a negligible difference to ERP waveforms.

The SPN was computed as the difference between reflection and random waves at posterior electrode cluster [PO7, O1, O2 and PO8]. SPN in the Repeated luminance condition was defined as Repeated luminance reflection – Repeated luminance random (averaging over black > black > black and white > white > white sequences). SPN in the Changing luminance condition was defined as Changing luminance reflection – Changing luminance random (averaging over black > white > black and white > black > white sequences). Three windows were chosen a-priori for statistical analysis of SPN priming: First window = 250–600 ms, Second window = 950–1300 ms, Third window = 1650–2000 ms.

SPN was analysed with repeated measures ANOVAs. There were 2 within subject factors [Sequence position (first, second third) X 2 Sequence type (Repeated luminance, Changing luminance)]. The assumption of sphericity was met (Mauchly's test $p > .159$) and none of SPNs in this analysis violated the assumption of normality according to Shapiro Wilk test ($p > .366$).

2.6 | Source waveform analysis (source level)

Source waveform analysis (implemented in BESA v. 7.0, MEGIS GmbH, Munich, Germany) was used to investigate the spatiotemporal dynamics of the SPN priming effect. Accurate localisation of cortical sources requires data with a large signal-to-noise ratio. Hence, the average difference wave (symmetry—random) was computed across the repeated and changing luminance conditions, thus producing the average waveform representing symmetry-specific activity.

The construction of a source dipole model requires that equivalent current dipoles (ECDs) are fitted to describe the 3-dimensional source currents from cortical regions contributing maximally to the observed data. To identify the number of contributing sources, principle component analysis (PCA) was used. In accordance with previous fMRI literature identifying the extrastriate cortex as being the origin of the SPN response (Keefe et al., 2018; Kohler et al., 2016; Sasaki et al., 2005; Tyler et al., 2005; Van Meel et al., 2019), two ECDs were fitted bilaterally within the extrastriate cortices. Classical LORETA analysis recursively applied (CLARA) was used as an independent source localisation method to confirm and adjust the locations of the ECDs. A source dipole model including bilateral ECDs within the extrastriate cortices explained 91.9% of the variance in the observed data. Since the PCA identified no other significantly contributing sources, no further ECDs were fitted. Finally, the orientation of the ECDs had to be determined. Due to differences in gyral anatomy between subjects, ECD orientation was determined on an individual subject basis but with the constraint of fixed ECD location between subjects. A 4-shell ellipsoid head volume conductor model was employed using the following conductivities (S/m = Siemens per meter): Brain = 0.33 S/m; Scalp = 0.33 S/m; Bone = 0.0042 S/m, Cerebrospinal Fluid = 1 S/m. Source waveforms for each experiment and condition were exported and analysed using repeated-measures ANOVAs.

3 | RESULTS

3.1 | ERP analysis (sensor level)

Grand average ERP waves are shown in Figure 3a. SPN difference waves are shown in Figure 3b. SPN amplitude in the three intervals are shown in Figure 3c.

All six SPNs in Figure 3c constitute significant brain responses to symmetry (amplitude < 0, one sample t tests, $p < .001$). As expected, SPN amplitude increased over the three presentations in both Repeated and Changing luminance conditions. Repeated measures ANOVA found a main effect of Sequence position ($F(2,42) = 3.624$, $p = .035$, $\eta_p^2 = 0.147$, linear contrast, $F(1,21) = 4.722$, $p = .041$, $\eta_p^2 = 0.184$), but no effect of Sequence type ($F < 1$), and no interaction ($F < 1$).

Additional analysis found no difference between SPNs generated by black and white reflections (collapsing over Sequence position and Sequence type, −1.89 vs. −1.97 microvolts, t (21) = 0.427, $p = .674$). This replicates previous work, where SPN amplitude was independent of luminance, contrast and colour, at least when magnitudes are matched in
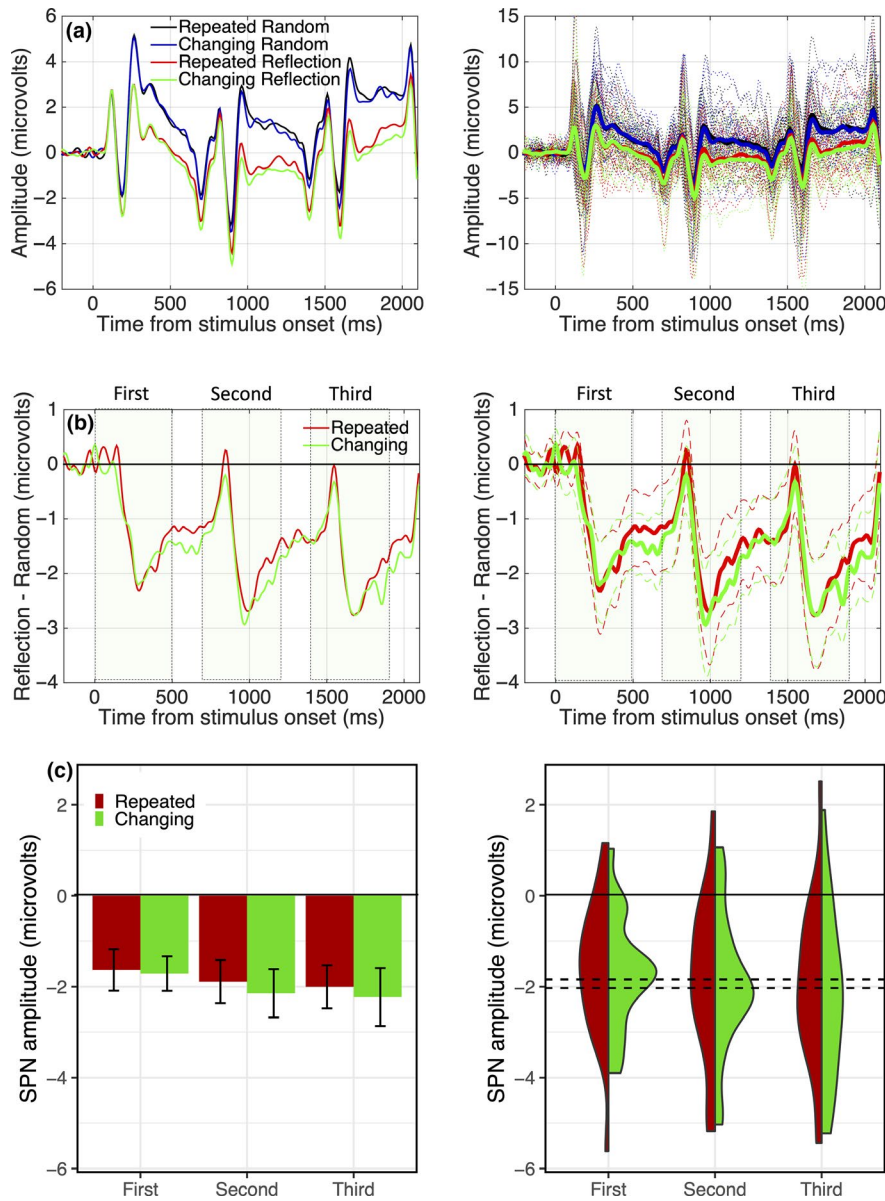
FIGURE 3 ERP results. Left and right columns show the same data; however, the right column has enriched visual representation of between-participant variability. (a) Left: Grand average ERP waves from posterior electrode cluster [PO7, O1, O2 and PO8]. Right: individual waves are presented behind the grand averages, and scale is expanded to accommodate this variance. (b) Left: SPN as a difference wave. The three intervals when the pattern was presented are marked. Right: 95% CI waves are presented behind the difference waves (dashed lines). (c) Left: SPN in first, second and third intervals (Error bars = 95% CI based on procedure of Morey, 2008). Right: a violin plot which represents density of individual participant data points. Black horizontal dashed lines indicate repeated and changing condition averages. SPN priming manifests as the widest bulge of the violin moving from above to below the line. Note that amplitude increases by around 0.5 microvolts in both repeated luminance (red) and changing luminance (green) conditions

reflected locations (Martinovic, Jennings, Makin, Bertamini, & Angelescu, 2018; Wright et al., 2018).

3.2 | Individual participant level analysis, effect size and power

The left column in Figure 3 shows ERP data in a standard format. The right column in Figure 3 shows the same ERP data, but with a richer visualization of between participant variation, as recommended by Rousselet, Foxe, and Bolam (2016). Note individual subject waves behind grand averages in Figure 3a (and the necessarily extended vertical scale to accommodate), 95% CI around difference waves in Figure 3b, and violin plots which represent distribution of individual-participant SPNs in Figure 3c.

Depending on condition, between 19/22 and 21/22 participants had an SPN (reflection < random). This is significantly more than the 11/22 = 0.5 expected by chance ($p = .001$, binomial test). Just 16/22 participants demonstrated an SPN priming effect (defined by a negative sequence position slope). This was only marginally greater than 0.5 ($p = .052$, binomial test). This marginal non-parametric effect suggests that our experiment was statistically underpowered. Furthermore, observed power for the significant parametric main effect of Sequence position was just 0.638, while the observed power of the linear contrast was just 0.545. However, SPN priming was replicated by Makin, Tyson-Carr, et al. (2020) in all the expected conditions (plus some unexpected conditions) across five experiments with 48 participants in each. Here effect size ranged from 0.110 to 0.290. We are thus confident that

SPN priming is a real effect, although future research that exploits SPN priming should obtain larger samples than our 22.

3.3 | Source waveform analysis (source level)

As discussed in Makin, Tyson-Carr, et al. (2020), the SPN priming effect is ambiguous when analysed at the sensor level. Does the increase in amplitude reflect increase in activation at extrastriate sources (as we assume) or later activation of additional dipoles elsewhere in the cortex? As in Makin, Tyson-Carr, et al. (2020), we ran additional source-level analysis to confirm that the observed SPN priming effect does indeed reflect increasing amplitude of the extrastriate symmetry response itself. This analysis also allowed us to assess hemispheric differences. This is important, because previous work has reported some right lateralization of the extrastriate symmetry response (Bertamini & Makin, 2014; Bona et al., 2015; Verma, Van der Haegen, & Brysbaert, 2013; Wright, Makin, & Bertamini, 2015).

A source dipole model was constructed comprised of two bilateral ECDs within the extrastriate regions. This model explained 91.9% of variance in the average difference wave across the repeated and changing conditions. Both the left ECD1 (Brodmann area 19; Talairach – x = −27.7, y = −61.9, z = 9.9) and the right ECD2 (Brodmann area 19; Talairach – x = 31.2, y = −61.8, z = −7.2) were located within the fusiform gyrus (see Figure 4a). The source waveforms for each ECD are illustrated in Figure 4b. It can be seen that the SPN priming effect is bilateral, and comparable in Repeated and Changing luminance conditions.

A three-way repeated measures ANOVA [Sequence type (Repeated luminance; Changing luminance) X Sequence position (First; Second; Third) X Hemisphere (Left ECD1; Right ECD2)] was carried out on the source waveforms.

There was a main effect of Sequence position ($F(1.371, 28.790) = 5.455$, $p = .018$, $\eta_p^2 = 0.206$). Although the right hemisphere response was numerically stronger, there were no other effects or interactions ($p \geq .096$).

4 | DISCUSSION

One branch of previous work has discovered SPN priming: SPN amplitude increases with repeated presentation of novel symmetrical exemplars (Figure 1). Another branch of previous work supports the non-selectivity hypothesis, and suggests that the extrastriate symmetry network pools element position information across low-level channels (Gheorghiu et al., 2016; Wright et al., 2018). We combined both branches of previous work and found new support for the non-selectivity hypothesis with SPN priming.

SPN priming was comparable when luminance polarity was repeated or changed in the triplet sequences. This suggests that black and white symmetries are not coded by independent neural systems.[2] Furthermore, source waveform analysis confirmed the SPN priming results at the source level and found no additional cortical sources. Therefore, SPN enhancement was due to increased activation *within* the extrastriate symmetry network. This is consistent with similar analysis in Makin, Tyson-Carr, et al. (2020).

TMS work has found that the disruption of LOC reduces symmetry repetition effects as measured behaviourally (Cattaneo, Mattavelli, Papagno, Herbert, & Silvanto, 2011). This also suggests repetition effects are mediated within the extrastriate symmetry network, in line with our source level analysis. However, the study by Cattaneo et al. (2011) raises some caveats here that require further discussion. In Cattaneo et al. (2011), participants were *slower* to discriminate target symmetry when it was congruent with the adaptor (e.g. Vertical > Vertical) than when it was

FIGURE 4 Source model. (a) Final source dipole model comprising two extrastriate sources. (b) Source waveforms for each ECD and mean amplitude within the defined intervals. Error bars = ± 1SD. (c) Mean scalp map for each sequence type and latency interval
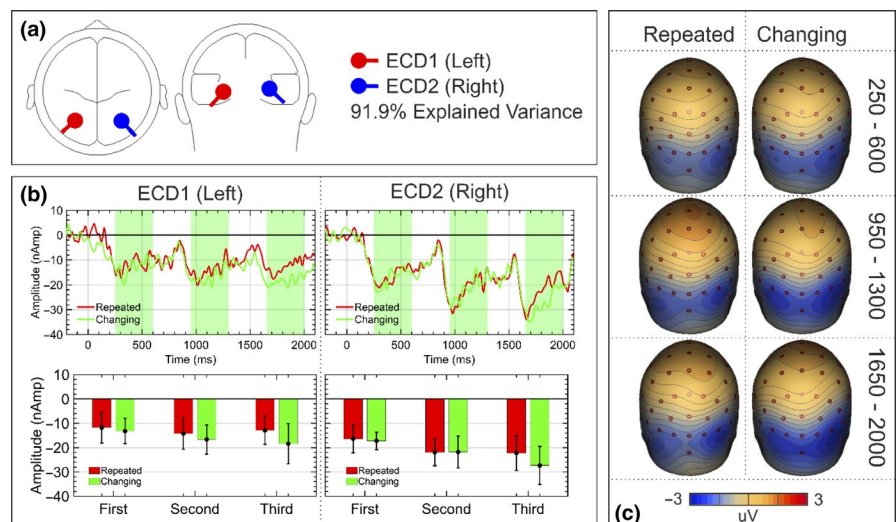
incongruent (Vertical > Horizontal). It is not clear why Cattaneo et al. (2011) found this when our results would predict the opposite (a congruence advantage). It could be that Cattaneo et al.'s participants had to inhibit the task-irrelevant adaptor, and this was more difficult when it matched the target orientation. In our study, the repeated trials were presented passively, so the symmetry response could accumulate without such cognitive complications.

It has been shown that SPN amplitude is similar for luminance defined (achromatic) and colour defined (isoluminant) stimuli when contrast greatly exceeds threshold (Martinovic et al., 2018). This suggests that the symmetry network is indifferent to luminance and colour, as the non-selectivity hypothesis claims. However, the ERP similarity demonstrated by Martinovic et al. (2018) is only an approximate indicator of neural similarity. Transfer of repetition effects, as demonstrated in the current study, is more convincing evidence for the non-selectivity hypothesis.

The non-selectivity hypothesis follows from other work. For instance, Tyler and Hardage (1996) found that second-order, polarity insensitive mechanisms are predominant during some symmetry discrimination tasks. Furthermore, filter models of symmetry perception can incorporate early half or full wave rectification (Dakin & Hess, 1997; Wilson & Wilkinson, 2002). This work also suggests that regularity coding should transcend element luminance polarity and predicts priming should transfer across changes in luminance polarity.

The current results are also in line with those of Clifford and Weston (2005), who found that Glass pattern aftereffects survive changes in luminance polarity. There are many similarities between neural coding of reflectional symmetry and Glass patterns (Rampone & Makin, 2020), so it is perhaps unsurprising that both are indifferent to element luminance polarity.

While the extrastriate symmetry network is not luminance polarity selective, we stress that it is sometimes *sensitive* to luminance polarity (mis)matching across the axis. This is revealed by experiments on anti-symmetry. As mentioned, some psychophysical work has found that anti-symmetry discrimination thresholds are elevated, especially when element density is high (Gheorghiu et al., 2016; Mancini et al., 2005; Wenderoth, 1996). The SPN is generated by anti-symmetry, but amplitude is reduced (Makin, Rampone, & Bertamini, 2020; Makin et al., 2016; Wright et al., 2018). Therefore, any future models of symmetry perception must account for both sensitivity to luminance polarity mismatching, AND the fact that extrastriate symmetry response is not gated by luminance polarity. The future theoretical challenge is to accommodate both these robust empirical findings.

Finally, we note that the visual effects of illumination and shading are typically unstable in real environments. When looking at a real object, the wavelengths reflected from its surfaces change quickly, while the spatial relationships between its parts change slowly. It is perhaps adaptive for visual object recognition mechanisms to be tuned to spatial relationships between parts, and ignore relatively superficial variability in luminance, contrast and colour.

CONFLICT OF INTEREST
The authors declare no conflict of interest.

AUTHOR CONTRIBUTIONS
Alexis Makin designed the experiment, analysed the results and wrote the manuscript. John Tyson-Carr collected some data and conducted the source localization analysis. Yiovanna Derpsch and Andrea Piovesan helped with data collection. Giulia Rampone assisted with EEG analysis and interpretation of results. Marco Bertamini programmed the stimuli, helped with interpretation of results and writing of the manuscript. All authors contributed to the final report.

PEER REVIEW
The peer review history for this article is available at https://publo ns.com/publo n/10.1111/ejn.14966

DATA AVAILABILITY STATEMENT
The experiments, stimuli and raw pre-processed EEG data are available on Open Science Framework (https://osf.io/2yjus/). We are happy for other researchers to use this material.

ORCID
Alexis D. J. Makin https://orcid.org/0000-0002-4490-7400

REFERENCES
Barlow, H. B., & Reeves, B. C. (1979). Versatility and absolute efficiency of detecting mirror symmetry in random dot displays. *Vision Research*, *19*(7), 783–793. https://doi.org/10.1016/0042-6989(79)90154-8

Bertamini, M., & Makin, A. D. J. (2014). Brain activity in response to visual symmetry. *Symmetry*, *6*, 975–996. https://doi.org/10.3390/sym6040975

Bertamini, M., Rampone, G., Oulton, J., Tatlidil, S., & Makin, A. D. J. (2019). Sustained response to symmetry in extrastriate areas after stimulus offset: An EEG study. *Scientific Reports*, *9*(1), 1–11. https://doi.org/10.1038/s41598-019-40580-z

Bertamini, M., Silvanto, J., Norcia, A. M., Makin, A. D. J., & Wagemans, J. (2018). The neural basis of visual symmetry and its role in mid- and high-level visual processing. *Annals of the*

New York Academy of Sciences, *1426*(1), 111–126. https://doi.org/10.1111/nyas.13667

Bona, S., Cattaneo, Z., & Silvanto, J. (2015). The causal role of the occipital face area (OFA) and lateral occipital (LO) cortex in symmetry perception. *The Journal of Neuroscience*, *35*(2), 731–738. https://doi.org/10.1523/JNEUROSCI.3733-14.2015

Bona, S., Herbert, A., Toneatto, C., Silvanto, J., & Cattaneo, Z. (2014). The causal role of the lateral occipital complex in visual mirror symmetry detection and grouping: An fMRI-guided TMS study. *Cortex*, *51*, 46–55. https://doi.org/10.1016/j.cortex.2013.11.004

Campbell, F. W., & Robson, J. G. (1968). Application of fourier analysis to the visibility of gratings. *The Journal of Physiology*, *197*(3), 551–566. https://doi.org/10.1113/jphysiol.1968.sp008574

Cattaneo, Z. (2017). The neural basis of mirror symmetry detection: A review. *Journal of Cognitive Psychology*, *29*(3), 259–268. https://doi.org/10.1080/20445911.2016.1271804

Cattaneo, Z., Mattavelli, G., Papagno, C., Herbert, A., & Silvanto, J. (2011). The role of the human extrastriate visual cortex in mirror symmetry discrimination: A TMS-adaptation study. *Brain and Cognition*, *77*(1), 120–127. https://doi.org/10.1016/j.bandc.2011.04.007

Clifford, C. W. G., & Weston, E. (2005). Aftereffect of adaptation to Glass patterns. *Vision Research*, *45*(11), 1355–1363. https://doi.org/10.1016/j.visres.2004.12.016

Dakin, S. C., & Herbert, A. M. (1998). The spatial region of integration for visual symmetry detection. *Proceedings of the Royal Society of London. Series B: Biological Sciences*, *265*(1397), 659–664. https://doi.org/10.1098/rspb.1998.0344

Dakin, S. C., & Hess, R. F. (1997). The spatial mechanisms mediating symmetry perception. *Vision Research*, *37*(20), 2915–2930. https://doi.org/10.1016/s0042-6989(97)00031-x

Dakin, S. C., & Watt, R. J. (1994). Detection of bilateral symmetry using spatial filters. *Spatial Vision*, *8*(4), 393–413. https://doi.org/10.1163/156856894x00071

Delorme, A., & Makeig, S. (2004). EEGLAB: An open source toolbox for analysis of single-trial EEG dynamics including independent component analysis. *Journal of Neuroscience Methods*, *134*(1), 9–21. https://doi.org/10.1016/j.jneumeth.2003.10.009

Driver, J., Baylis, G. C., & Rafal, R. D. (1992). Preserved figure-ground segregation and symmetry perception in visual neglect. *Nature*, *360*(6399), 73–75. https://doi.org/10.1038/360073a0

Gheorghiu, E., Kingdom, F. A. A., Remkes, A., Li, H.-C.-O., & Rainville, S. (2016). The role of color and attention-to-color in mirror-symmetry perception. *Scientific Reports*, *6*, 29287. https://doi.org/10.1038/srep29287

Glass, L. (1969). Moire effect from random dots. *Nature*, *223*, 578–580.

Jacobsen, T., & Höfel, L. (2003). Descriptive and evaluative judgment processes: Behavioral and electrophysiological indices of processing symmetry and aesthetics. *Cognitive Affective & Behavioral Neuroscience*, *3*(4), 289–299. https://doi.org/10.3758/CABN.3.4.289

Julesz, B., & Chang, J.-J. (1979). Symmetry perception and spatial-frequency channels. *Perception*, *8*(6), 711–718. https://doi.org/10.1068/p080711

Jung, T. P., Makeig, S., Humphries, C., Lee, T. W., McKeown, M. J., Iragui, V., & Sejnowski, T. J. (2000). Removing electroencephalographic artifacts by blind source separation. *Psychophysiology*, *37*(2), 163–178. https://doi.org/10.1111/1469-8986.3720163

Keefe, B. D., Gouws, A. D., Sheldon, A. A., Vernon, R. J. W., Lawrence, S. J. D., McKeefry, D. J., … Morland, A. B. (2018). Emergence of symmetry selectivity in the visual areas of the human brain: fMRI responses to symmetry presented in both frontoparallel and slanted planes. *Human Brain Mapping*, *39*(10), 3813–3826. https://doi.org/10.1002/hbm.24211

Kim, J. G., Biederman, I., Lescroart, M. D., & Hayworth, K. J. (2009). Adaptation to objects in the lateral occipital complex (LOC): Shape or semantics? *Vision Research*, *49*(18), 2297–2305. https://doi.org/10.1016/J.VISRES.2009.06.020

Koffka, P. J. (1935). *Priciples of Gestalt Psychology*. New York: Harcourt, Brace & Company.

Kohler, P., Clarke, A., Yakovleva, A., Liu, Y., & Norcia, A. M. (2016). Representation of maximally regular textures in human visual cortex. *The Journal of Neuroscience*, *36*(3), 714–729. https://doi.org/10.1523/JNEUROSCI.2962-15.2016

Kourtzi, Z., & Kanwisher, N. (2001). Representation of perceived object shape by the human lateral occipital complex. *Science*, *293*(5534), 1506–1509. https://doi.org/10.1126/science.1061133

Mach, E. (1886). *The analysis of sensations and the relation of the phsysical to the psychical*. New York: Dover.

Makin, A. D. J., Rampone, G., & Bertamini, M. (2020). Symmetric patterns with different luminance polarity (anti-symmetry) generate an automatic response in extrastriate cortex. *European Journal of Neuroscience*, *51*(3), 922–936. https://doi.org/10.1111/ejn.14579

Makin, A. D. J., Rampone, G., Morris, A., & Bertamini, M. (2020). The formation of symmetrical gestalts is task independent, but can be enhanced by active regularity discrimination. *Journal of Cognitive Neuroscience*, *32*(2), 353–366. https://doi.org/10.1162/jocn_a_01485

Makin, A. D. J., Tyson-Carr, J., Rampone, G., Derpsch, Y., & Bertamini, M. (2020). PsyArXiv Preprints | A new ERP repetition paradigm to assess independence of regularity representations in the extrastriate cortex. Retrieved May 28, 2020, from https://psyarxiv.com/a8n6b/.

Makin, A. D. J., Wilton, M. M., Pecchinenda, A., & Bertamini, M. (2012). Symmetry perception and affective responses: A combined EEG/EMG study. *Neuropsychologia*, *50*(14), 3250–3261. https://doi.org/10.1016/j.neuropsychologia.2012.10.003

Makin, A. D. J., Wright, D., Rampone, G., Palumbo, L., Guest, M., Sheehan, R., … Bertamini, M. (2016). An electrophysiological index of perceptual goodness. *Cerebral Cortex*, *26*, 4416–4434. https://doi.org/10.1093/cercor/bhw255

Mancini, S., Sally, S. L., & Gurnsey, R. (2005). Detection of symmetry and anti-symmetry. *Vision Research*, *45*(16), 2145–2160. https://doi.org/10.1016/j.visres.2005.02.004

Martinovic, J., Jennings, B. J., Makin, A. D. J., Bertamini, M., & Angelescu, I. (2018). Symmetry perception for patterns defined by color and luminance. *Journal of Vision*, *18*(8), 1–24. https://doi.org/10.1167/18.8.4

Morey, R. D. (2008). Confidence intervals from normalized data: A correction to Cousineau (2005). *Tutorials in Quantitative Methods for Psychology*, *4*(2), 61–64. https://doi.org/10.20982/tqmp.04.2.p061

Norcia, A. M., Candy, T. R., Pettet, M. W., Vildavski, V. Y., & Tyler, C. W. (2002). Temporal dynamics of the human response to symmetry. *Journal of Vision*, *2*(2), 132–139. https://doi.org/10.1167/2.2.1

Osorio, D. (1996). Symmetry detection by categorization of spatial phase, a model. *Proceedings of the Royal Society B: Biological Sciences*, *263*(1366), 105–110. https://doi.org/10.1098/rspb.1996.0017

Peirce, J. W. (2007). PsychoPy - Psychophysics software in Python. *Journal of Neuroscience Methods*, *162*(1–2), 8–13. https://doi.org/10.1016/j.jneumeth.2006.11.017

Poirier, F., & Wilson, H. R. (2010). A biologically plausible model of human shape symmetry perception. *Journal of Vision*, *10*(1), https://doi.org/10.1167/10.1.9

Rainville, S. J. M., & Kingdom, F. A. A. (2000). The functional role of oriented spatial filters in the perception of mirror symmetry — psychophysics and modeling. *Vision Research*, *40*(19), 2621–2644. https://doi.org/10.1016/S0042-6989(00)00110-3

Rampone, G., & Makin, A. D. J. (2020). Electrophysiological responses to regularity show specificity to global form: The case of Glass patterns. *European Journal of Neuroscience*, *52*(3), 3032–3046. https://doi.org/10.1111/ejn.14709

Rousselet, G. A., Foxe, J. J., & Bolam, J. P. (2016). A few simple steps to improve the description of group results in neuroscience. *European Journal of Neuroscience*, *44*(9), 2647–2651. https://doi.org/10.1111/ejn.13400

Sasaki, Y., Vanduffel, W., Knutsen, T., Tyler, C. W., & Tootell, R. (2005). Symmetry activates extrastriate visual cortex in human and nonhuman primates. *Proceedings of the National Academy of Sciences of the United States of America*, *102*(8), 3159–3163. https://doi.org/10.1073/pnas.0500319102

Treder, M. S. (2010). Behind the looking glass: A review on human symmetry perception. *Symmetry*, *2*, 1510–1543. https://doi.org/10.3390/sym2031510

Tyler, C. W., Baseler, H. A., Kontsevich, L. L., Likova, L. T., Wade, A. R., & Wandell, B. A. (2005). Predominantly extra-retinotopic cortical response to pattern symmetry. *NeuroImage*, *24*(2), 306–314. https://doi.org/10.1016/j.neuroimage.2004.09.018

Tyler, C. W., & Hardage, L. (1996). Mirror symmetry detection: Predominance of second-order pattern processing throughout the visual field. In C. W. Tyler (Ed.), *Human Symmetry Perception and Its Computational Analysis* (pp. 157–171). Utrecht: Lawrence Erlbaum.

van der Helm, P. A., & Leeuwenberg, E. L. J. (1996). Goodness of visual regularities: A nontransformational approach. *Psychological Review*, *103*(3), 429–456. https://doi.org/10.1037/0033-295x.103.3.429

Van Meel, C., Baeck, A., Gillebert, C. R., Wagemans, J., & Op de Beeck, H. P. (2019). The representation of symmetry in multi-voxel response patterns and functional connectivity throughout the ventral visual stream. *NeuroImage*, *191*, 216–224. https://doi.org/10.1016/j.neuroimage.2019.02.030

Verma, A., Van der Haegen, L., & Brysbaert, M. (2013). Symmetry detection in typically and atypically speech lateralized individuals: A visual half-field study. *Neuropsychologia*, *51*(13), 2611–2619. https://doi.org/10.1016/j.neuropsychologia.2013.09.005

Wagemans, J., Van Gool, L., Swinnen, V., & Vanhorebeek, J. (1993). Higher-order structure in regularity detection. *Vision Research*, *33*(8), 1067–1088. https://doi.org/10.1016/0042-6989(93)90241-n

Wenderoth, P. (1996). The effects of the contrast polarity of dot-pair partners on the detection of bilateral symmetry. *Perception*, *25*(7), 757–771. https://doi.org/10.1068/p250757

Wilson, H. R., & Wilkinson, F. (2002). Symmetry perception: A novel approach for biological shapes. *Vision Research*, *42*(5), 589–597. https://doi.org/10.1016/S0042-6989(01)00299-1

Wright, D., Makin, A. D. J., & Bertamini, M. (2015). Right-lateralized alpha desynchronization during regularity discrimination: Hemispheric specialization or directed spatial attention? *Psychophysiology*, *52*, 638–647. https://doi.org/10.1111/psyp.12399

Wright, D., Mitchell, C., Dering, B. R., & Gheorghiu, E. (2018). Luminance-polarity distribution across the symmetry axis affects the electrophysiological response to symmetry. *NeuroImage*, *173*, 484–497. https://doi.org/10.1016/J.NEUROIMAGE.2018.02.008